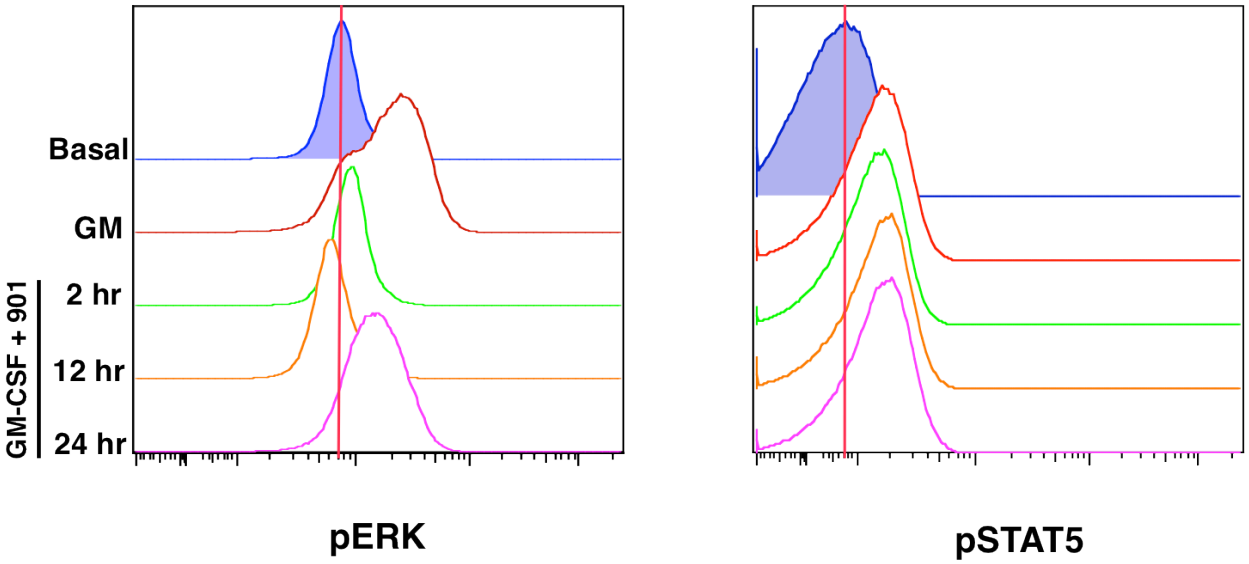

Supplemental Figure 1. PD0325901 inhibits MEK in vivo. Mice were treated with 5 mg/kg/day of PD0325901 (901) for 5 days, then euthanized 2,12, or 24 hours after the final dose. Phosphorylated ERK and STAT5 (pERK/pSTAT5) levels were measured by flow cytometry in $Mac1^{+}$ bone marrow cells after stimulation with a saturating dose of GM-CSF (10 ng/mL).

Supplemental Figures

Chang *et al.*

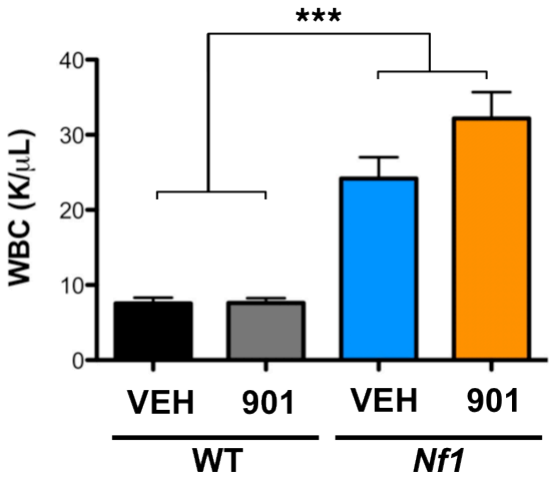

Supplemental Figure 2. White blood cell (WBC) counts at study entry in *Mx1-Cre; Nf1$^{flox/flox}$ (Nf1)* and wild-type (WT) mice. *Mx1-Cre; Nf1$^{flox/flox}$* mice develop MPN by 6-months, which is characterized by elevated white blood cell counts compared to control mice ($P < 0.0001$). WBC counts were similar in *Nf1* mutant mice that were randomly assigned to receive PD0325901 (901) or the control vehicle (VEH) (P = ns). The error bars indicate standard error of the mean (n = 17-18 per group).

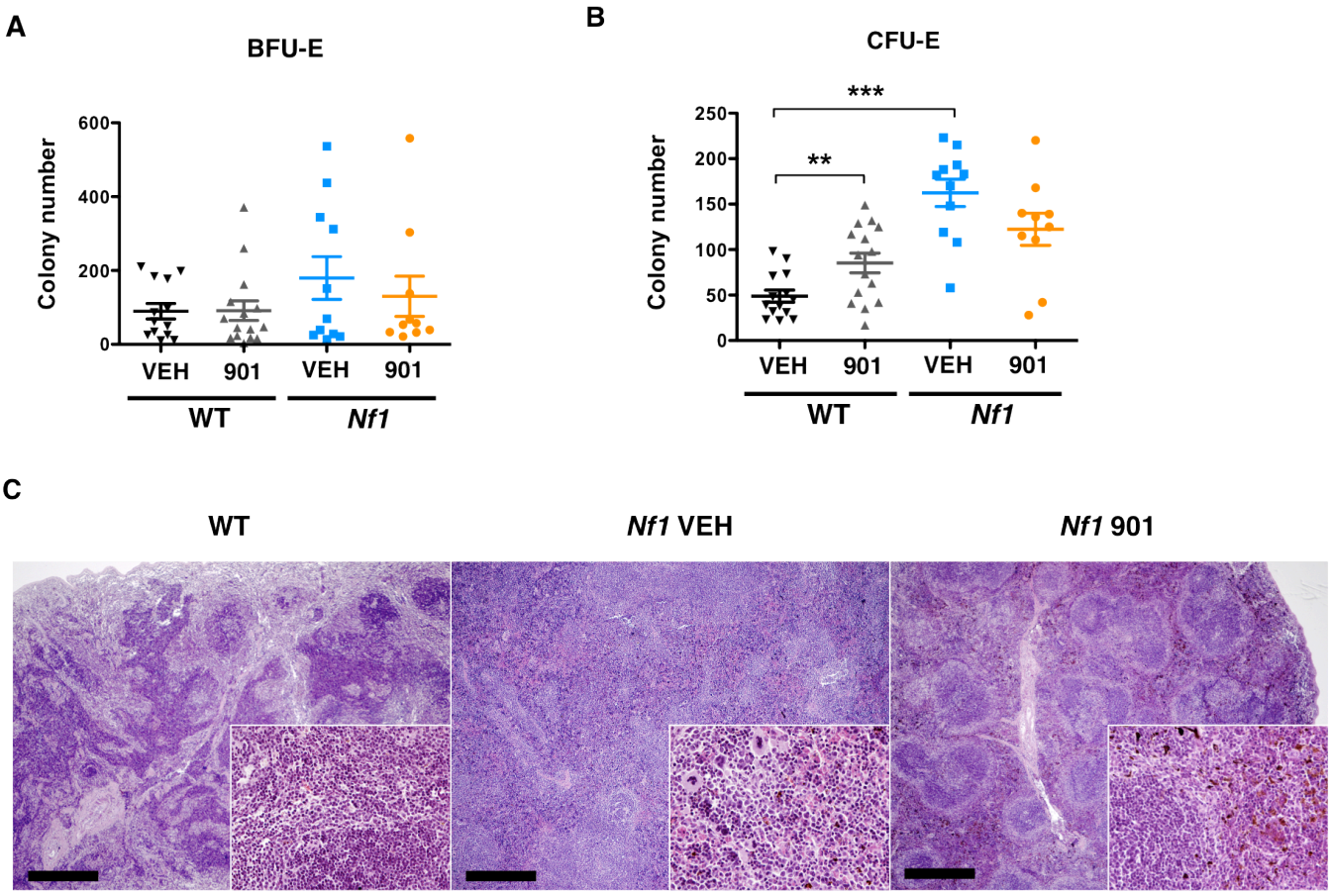

Supplemental Figure 3. Bone marrow erythroid progenitor growth and splenic morphology from *Mx1-Cre; Nf1*$^{flox/flox}$ (*Nf1*) and wild type (WT) at the end of the trial. (A,B) Bone marrow cells from *Mx1-Cre; Nf1*$^{flox/flox}$ and WT mice that received 901 or the control vehicle were grown in methylcellulose with a saturating concentration of erythropoietin (100 ng/mL). There were no statistically significant differences in the number of burst forming unit erythroid (BFU-E) colonies that formed from 10^5 bone marrow mononuclear cells in any of the 4 study groups (left panel). The frequency of bone marrow CFU-E colonies was significantly higher in vehicle-treated *Nf1* mice compared to vehicle-treated WT mice ($P = 0.0001$). Interestingly, WT mice that were treated with 901 showed a modest increase in the frequency of CFU-E progenitors at the end of the trial ($P = 0.0088$), which likely reflects a stress response to chronic MEK inhibition. By contrast, treatment reduced the CFU-E numbers in *Nf1* mutant mice, but this difference did not achieve statistical significance. Symbols represent individual samples; horizontal bars represent mean; and error bars show SEM. **(C)** Representative hematoxylin/eosin-stained sections from WT and *Nf1* mutant mice treated with vehicle or 901. The vehicle-treated *Nf1* mutant spleen shows markedly expanded red pulp with increased myelopoiesis and loss of normal splenic architecture. Comparatively, spleens of *Nf1* mutant mice treated with 901 demonstrate a reduction in red pulp with decreased myeloid infiltration (scale bar = 500 μm). Inset demonstrates mixed myeloid hyperplasia in vehicle-treated *Nf1* mutant spleen that is decreased in 901 treated animals (scale bar = 100 μm).

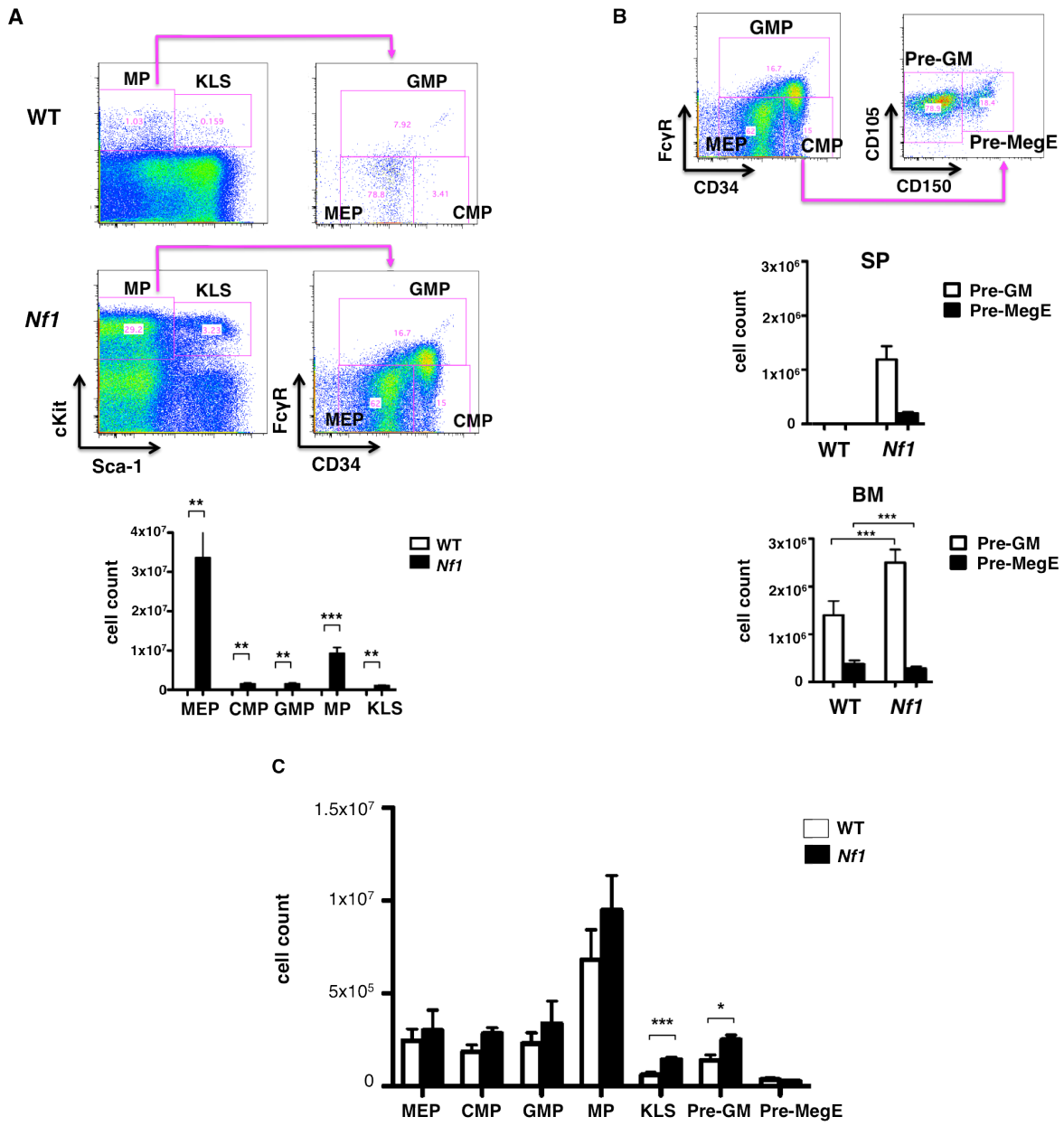

Supplemental Figure 4. Consequences of *Nf1* Inactivation on Hematopoietic Populations. The frequency of each population was determined by flow cytometry. **(A)** Representative immunophenotypic analysis of splenocytes isolated from wild-type (WT) and *Mx1-Cre; Nf1$^{flox/flox}$ (Nf1)* mice. Cells gated for c-kit^{+}, Lin$^{-/lo}$, Sca1^{-} (KLS) expression are shown. Bar graphs depict the absolute numbers of each progenitor population in the spleens of WT and *Nf1* mutant mice. Asterisks indicate significant differences between groups (**P < 0.01, *** P < 0.0001). **(B)** Characterization of intermediate myeloid progenitors. Gating protocol for identifying Pre-GM and Pre-MegE populations from spleen and bone marrow (top panel), total numbers of pre-GM (white) and pre-MegE (black) in the spleens and bone marrows of WT and *Nf1* mutant mice (middle and bottom panels). Asterisks indicate significant differences between these groups (***P < 0.0001). **(C)** Total numbers of immature bone marrow progenitors in WT and *Nf1* mice. *Nf1* mutant mice showed significant increases in bone marrow KLS and pre-GM populations compared to WT animals (*P < 0.05; *** P < 0.0001). All error bars show SEM (n=6-10 per group). Nucleated bone marrow and spleen cells were stained with the following antibodies (eBiosciences, Biolegend, AbCam and BD Biosciences): lineage markers (unconjugated CD3, CD4, CD5, CD8, B220, Mac1 or Gr1), FITC-CD34, Alx700-FcγR, APC-Sca1, APC/Cy7–C-kit, PE-CD150, Pacific Blue CD105 for stem and progenitor cells, and FITC-CD71, PE-Ter119 for erythroid precursor

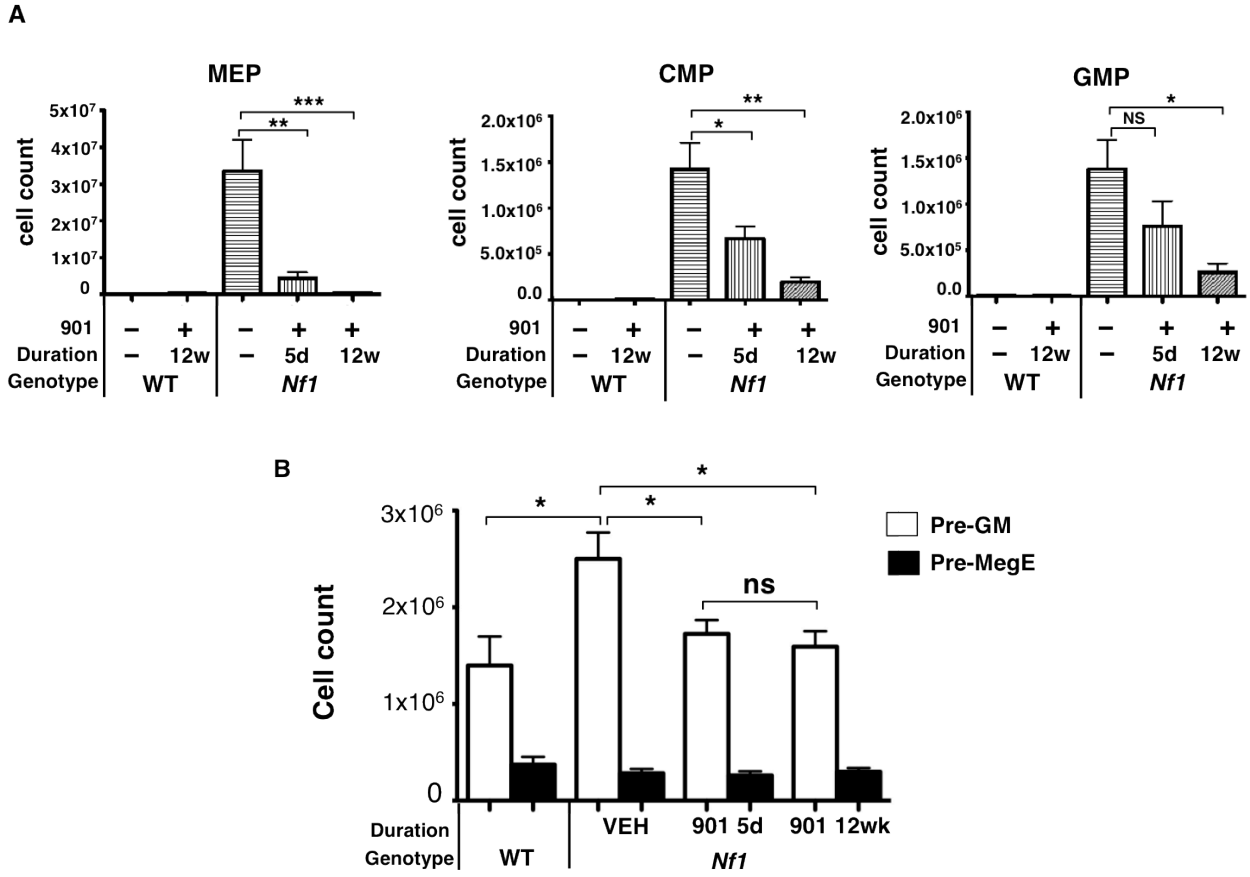

Supplemental Figure 5. Treatment with PD0325901 reduces pre-GM progenitor numbers and normalizes the ratios of pre-GM to pre-MegE cells in the bone marrows of *Mx1-Cre, Nf1$^{flox/flox}$ (Nf1)* mice. (A) Total numbers of splenic myeloid progenitor cells in WT and *Nf1* mutant mice treated with 901 for 5 days or 12 weeks. MEP, megakaryocyte-erythroid progenitors; CMP, common myeloid progenitors; GMP, granulocyte-macrophage progenitors. **(B)** Total numbers of bone marrow pre-GM (white bars) and pre-MegE (black bars) progenitors in untreated WT and *Nf1* mice, and of *Nf1* mutant mice that received 901 for 5 days or 12 weeks. Note that the pre-GM population was selectively reduced after 5 days of 901 treatment and that this difference persisted at 12 weeks. All error bars show SEM (n=5-10 per group), * $P < 0.05$.

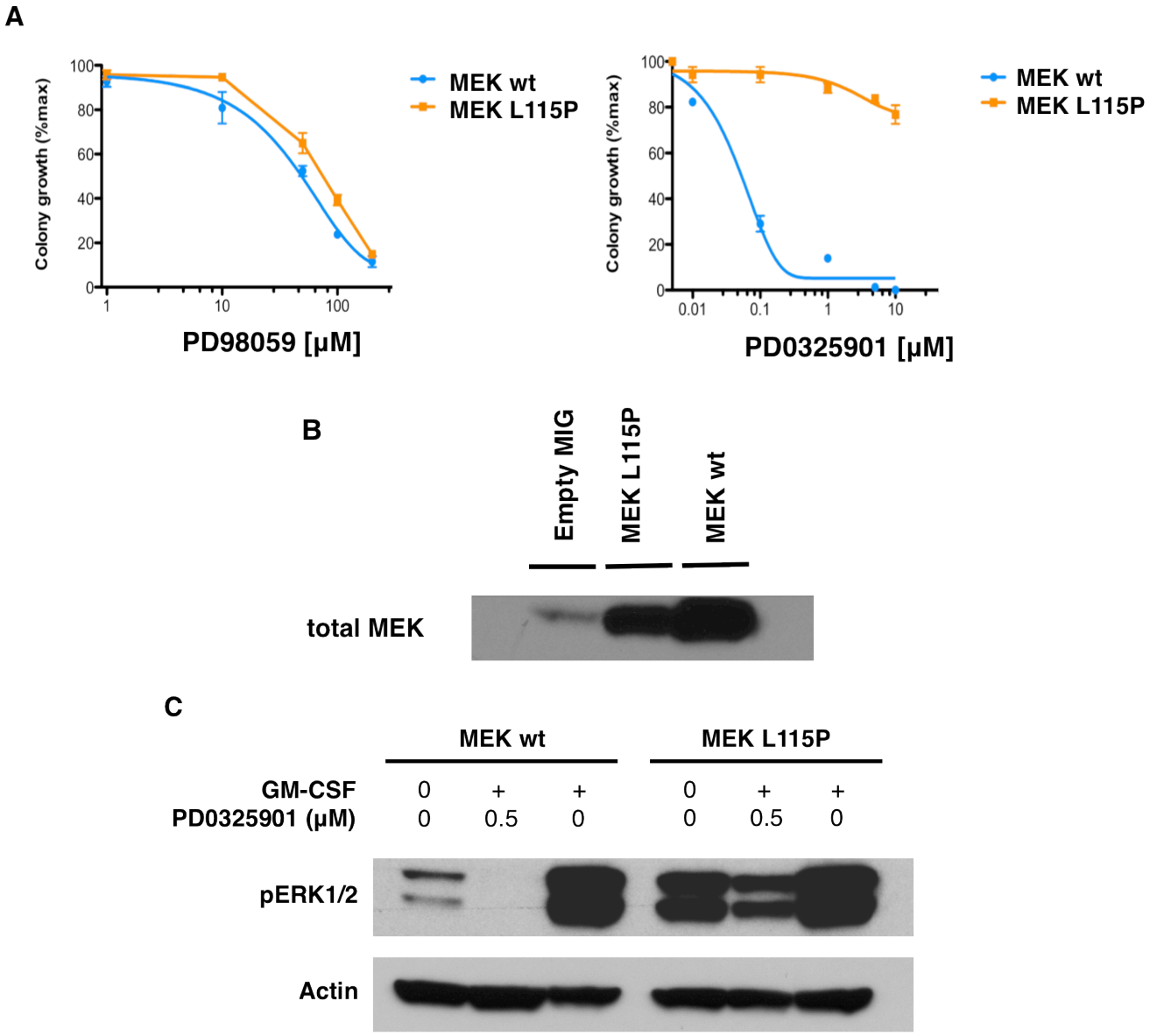

Supplemental Figure 6. MEK inhibition underlies the biologic effects of PD0325901 in primary hematopoietic cells. Mouse fetal liver cells were transduced with retroviral vectors expressing a GFP marker and either wild-type (wt) MEK or a MEK mutant with a substitution (L115P) in the allosteric CI-1040/901 binding pocket. GFP^+ cells that were isolated by sorting were analyzed to assess CFU-GM growth and were differentiated into macrophages for biochemical studies. **(A)** CFU-GM growth over a range of PD98059 (left) or 901 (right) concentrations. Note that PD98059, a MEK inhibitor structurally unrelated to 901, demonstrates dose-dependent inhibition of CFU-GM growth that is independent of the L115P substitution. By contrast, CFU-GM expressing the L115P mutant are resistant to growth inhibition by 901. **(B)** Western blot analysis of macrophages differentiated from GFP^+ fetal liver cells demonstrates over-expression of both MEK proteins with the wt protein expressed at somewhat higher levels. **(C)** Levels of pERK1/2 in macrophages expressing MEK wt or MEK L115P following 15 minute incubation with PD0325901 at 0.5 μM. This dose was selected based on the strong inhibitory effects seen in the CFU-GM assay. Note that pERK levels are higher in starved cells expressing L115P MEK, which is likely due to higher basal kinase activity. Importantly, cells expressing this mutant protein maintain ERK phosphorylation in the presence of 901 while cells expressing wt MEK do not.

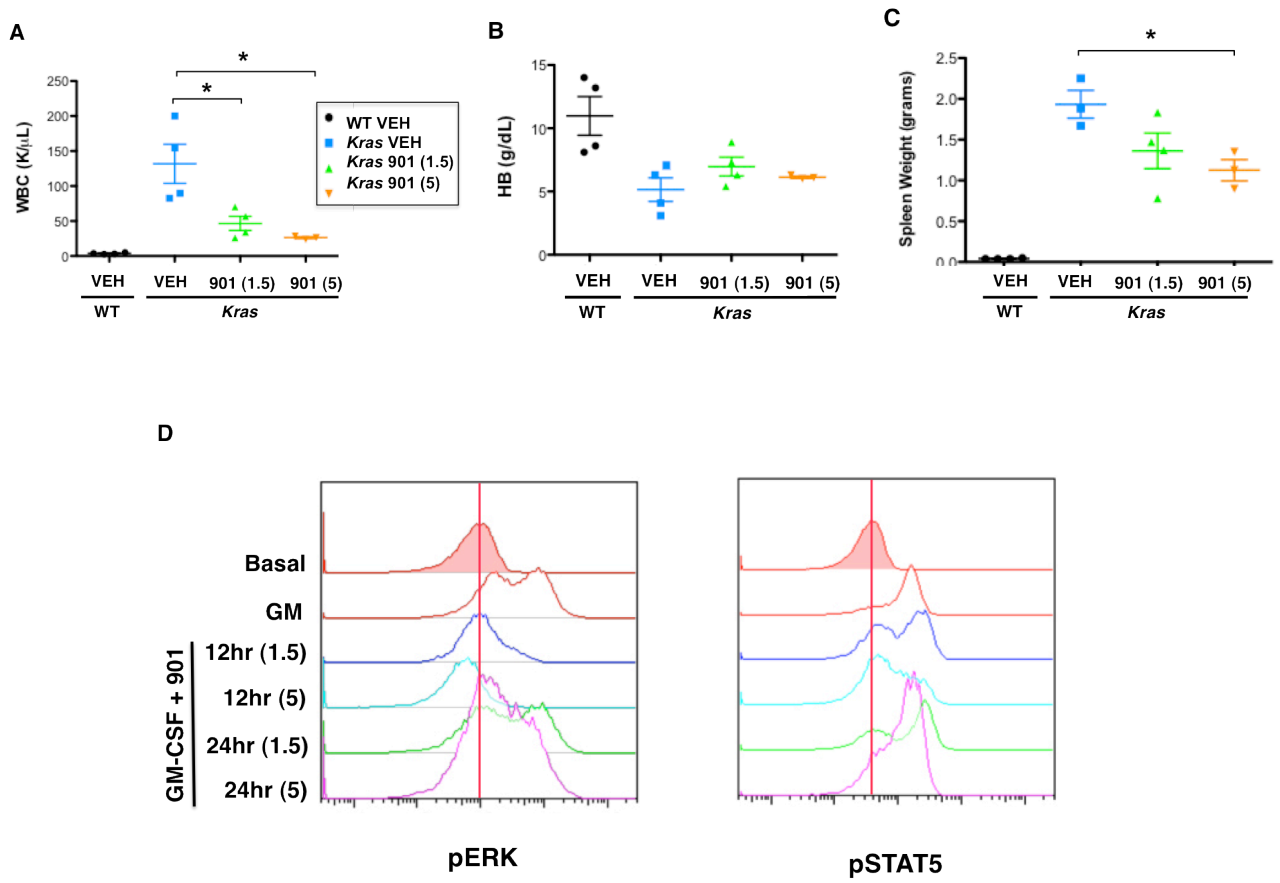

Supplemental Figure 7. Preclinical efficacy and pharmacodynamics of PD0325901 at doses of 1.5 and 5 mg/kg/day in *Mx1-Cre, Kras^{G12D}* mice with MPN. (A) White blood cell (WBC) counts, **(B)** hemoglobin (Hb) concentrations, and **(C)** spleen weights of wild-type (WT) and *Mx1-Cre, Kras^{G12D}* (*Kras*) mice after treatment with either 1.5 mg/kg/day (green), or 5 mg/kg/day (orange) of 901 or control vehicle (blue) for 8 weeks. Symbols represent individual samples; horizontal bars represent mean; and error bars show SEM (n=3–4 per group), $*P < 0.05$. Mice treated with either dose of 901 had similar responses to treatment with no significant differences in WBC, Hb, or spleen weight at the end of the trial. **(D)** *Kras* and WT mice that received either 1.5 mg/kg/day or 5 mg/kg/day of 901 were euthanized 12 or 24 hours after the 5th daily drug dose. Phosphorylated ERK (pERK; left panel) and STAT5 (pSTAT5; right panel) levels were assessed by flow cytometry in bone marrow pre-GM progenitors after stimulation with GM-CSF (10 ng/mL). This pharmacodynamic analysis revealed inhibition of the ability of GM-CSF to increase pERK levels that was sustained for 12 hours at both 901 dose levels. Note that the cells regain responsiveness after 24 hours with evidence of some persistent inhibition at the 5 mg/kg dose only.

Full Unedited Gel for **Figure 1F (below)**

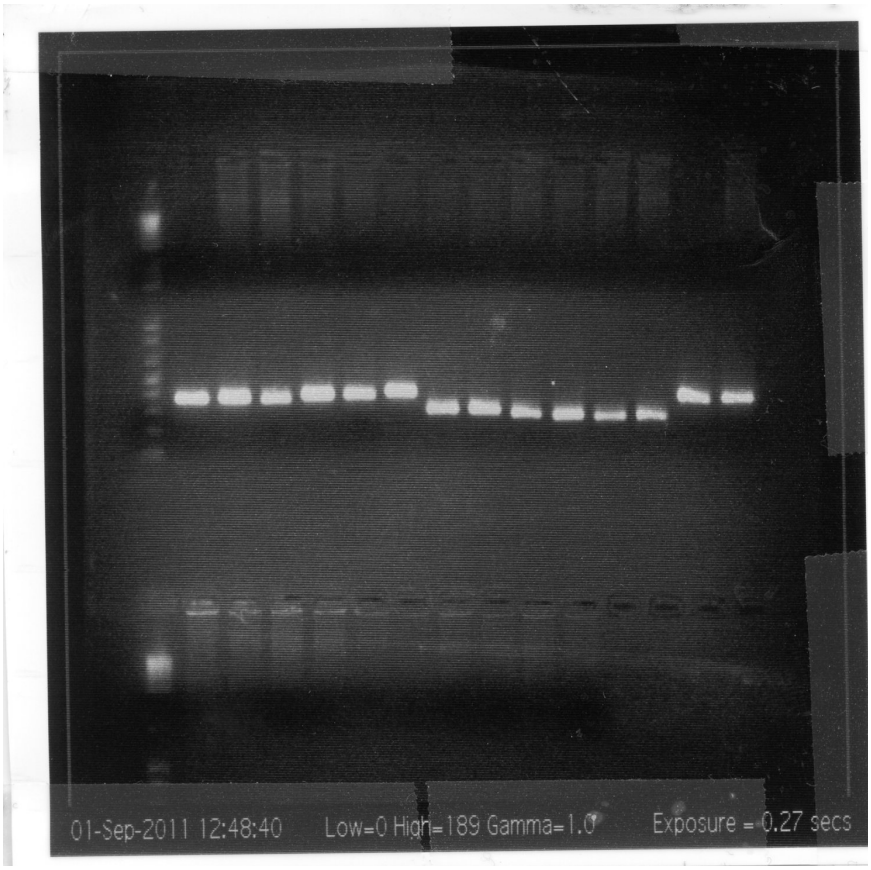

F

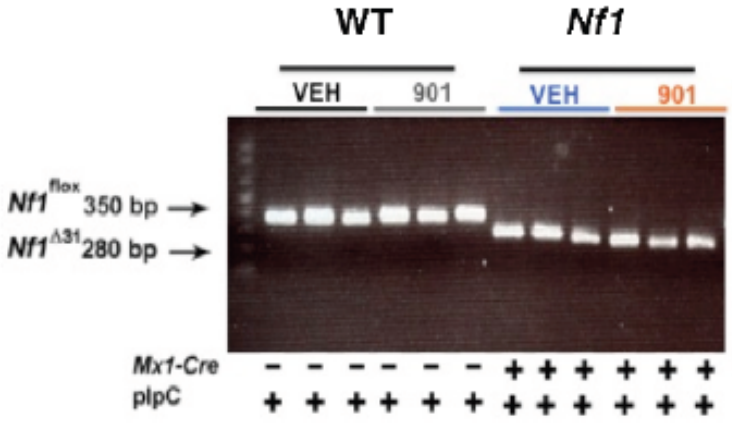

Full Unedited Gel for **Supplemental Figure 6B (below)**

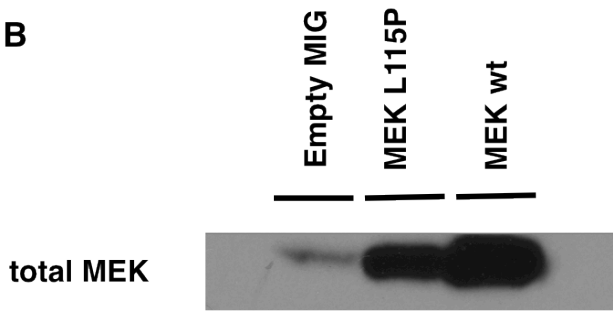

Full Unedited Gel for **Supplemental Figure 6C (below)**